Colloid Science

SAXS Study of core-shell colloids*)

D. Beyer, W. Lebek, W.-D. Hergeth and K. Schmutzler

Technical University Merseburg, Department of Physics, Merseburg, GDR

Abstract: Polymeric core-shell systems were produced by a two-stage emulsion polymerization technique under fixed conditions: i) monodisperse seed latex with a sufficiently high particle number; ii) starved monomer-II addition; iii) water-soluble initiator; iv) incompatibility of core and shell polymer. From electron micrographs, it is not possible to determine where the second polymer is located within these two-stage emulsion polymers. The internal structure of the particles can be detected by small-angle x-ray scattering. The results indicate that; i) the emulsion polymerization process takes place in a small surface layer region of the seed particles, and ii) a small interfacial layer exists between the core and shell polymer.

Key words: Polymer colloids; emulsion polymerization; core-shell structure; small angle x-ray scattering

Introduction

Emulsion polymerization is a well-known technique for producing dispersions with a core-shell structure of polymer particles. There are some advantages and applications of polymer dispersions produced by this technique: i) The modification of the interfacial properties of emulsion polymers by preparing well-defined core-shell structures affords the improvement of film properties of the latex. ii) Investigations of the formation of core-shell structures give information about the topo-chemistry of the reaction during the period of particle growth, and about adsorption and absorption phenomena. iii) The polymers with core-shell structures are perfect model systems in material science because of the regular distribution of their components and the simple spherical geometry of the system.

One of the main problems in investigating core-shell latex particles is the detection of this type of internal structure. The direct observation by electron microscopy does not permit any conclusive evidence for the formation of shells around cores. This can be only partially overcome by the selective staining of the different components [1, 2]. Okubo et al. [3] applied a soap titration method in order to estimate the particle morphology indirectly. Wide-angle light scattering was used by Ford et al. [4] as the principal probe to examine the core-shell structure proposed for certain alkali-swellable acrylic acid acrylate ester copolymer latexes. However, the authors only obtained "marginal evidence for a shell of low refractive index, and of ill-defined extent". The application of small-angle neutron scattering is a very reliable method of obtaining a core-shell structure, but it is also very expensive and time-consuming [5, 6]. Therefore, the aim of this publication was to study the application of a more suitable "structure-sensitive" method that; i) is easy for handling, and ii) gives conclusive evidence of the core-shell structure. The method used was small-angle x-ray scattering (SAXS). So far as the authors know, there is no other SAXS study of core-shell latex systems in the literature.

---

*) Part 6 of "Polymerizations in the Presence of Seeds"

I. Experimental

The polymerizations were carried out as two-stage reactions in an all-glass reaction vessel, constantly stirred (250 r.p.m.), at a constant temperature. The monodisperse seed latexes (first stage) were prepared using recipes and procedures developed by Zecha [7]. The polymer volume fraction of these seed latexes was approximately 0.10. In the second stage, 22 g of the PS seed latex were removed from the tank, charged into the reaction vessel, and heated, stirring continuously, to the reaction temperature (70 °C). The initiator (0.13 g $K_2S_2O_8$) was dissolved in 8 g water, heated to the reaction temperature, and added to the reaction mixture. The dropwise addition of the second monomer (methyl methacrylate) was carried out with a monomer addition rate below the maximum reaction rate of the homo-emulsion polymerization under the same conditions (i.e., monomer starved addition: ca. 25 μl/min). The second stage was polymerized without any further addition of the emulsifier.

The monomers used were technical products. They were applied after conventional cleaning. All other ingredients (potassium persulfate, sodium dodecylsulfate, borax) were of analytical grade. The dispersion medium was twice-distilled water. The monomer conversion and polymer weight fractions were determined gravimetrically. Transmission electron micrographs were obtained from diluted samples deposited on a thin carbon layer on a copper grid in a BS 613 electron microscope (Tesla, CSFR), without further staining.

The SAXS-intensity profile, as a function of the wave vector h = 4 π/λ $\sin\Theta/2$ (where λ and Θ are the wave-length and scattering angle, respectively), was measured using a Kratky camera. The $Cu_{K\alpha}$-radiation (λ =1.54 Å) was selected by a total reflection method with a flat glass plate. The height of the entrance slit was 25 μm and that of the counter slit was 75 μm. The width of both slits was 10 mm. The experimental counts, as a function of scattering angle, were corrected for scattering of the empty equipment and were slightly treated using cubic spline functions. The desmearing procedure for slit height correction is a computer program based on the general discussion in [8]. This procedure does not change the position of the extrema of the scattering curve in our experiments.

III. Results and Discussion

In Fig. 1, the monodispersity of the PS seed latex particles can be seen: Polydispersity ratio $\overline{P}_v$ = $\overline{R}_W/\overline{R}_N$ = 1.021 (see also Table 1). $\overline{R}_W$ and $\overline{R}_N$ are the weigth average and the number average particle radius, respectively.

The seeded polymerizations were carried out applying a seed latex particle number which is high enough to prevent the formation of separate particles during the second stage of the reaction. This minimal seed latex particle number N_I can be estimated following a proposition by Schmutzler [9]:

$$N_I^2 \gtrsim \frac{3 \cdot k_{11}}{8\pi \cdot k_{12}^2 \cdot r_0^3 \cdot \rho_T} \cdot \frac{dM}{dt} \qquad (1)$$
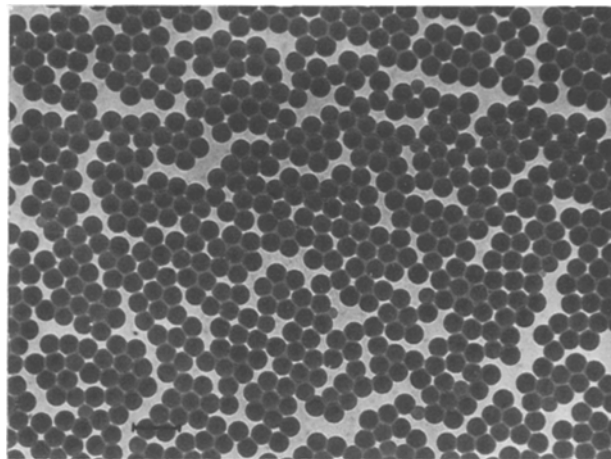

Fig. 1. PS seed latex particles (the bar indicates 250 nm)

where k_{11} and k_{12} describe the coagulation rate constants between primary particles and between primary particles and latex particles, respectively. r_0 and ρ_T are the radius and the density of primary particles and dM/dt is the monomer conversion per unit time of the second stage of polymerization (for a detailed discussion of this see ref. [9]). Condition 1 was experimentally verified using polymer latexes [9, 10, 11] and inorganic quartz powder filler particles as seeds [12]. Under these circumstances, additional experimental conditions for the formation of homogeneous polymeric shells around polymeric seeds can be summarized as follows [11, 13]:

– use of water soluble initiator
– monomer II addition under starved conditions
– higher water solubility of monomer II than that of monomer I
– incompatibility of the two polymers.

With these conditions, the emulsion polymerization of methyl methacrylate, in the presence of monodisperse PS latex particles, produces spherical polymer particles (containing both polymers) with a narrow range of size distribution ($\overline{P}_V$ = 1.051). The particle radius increases according to the addition of the second monomer. However, from the electron micrographs, it is impossible to determine where the second polymer is located within these particles. Ultra-thin cross-sections of the samples as well as selective staining techniques did not give a better insight into the particle structure. Therefore, SAXS experiments were carried out in order to overcome the difficulties by direct observations with electron microscopy.

The x-ray scattering intensity observed in the experiments of this study is directly determined by the scattering amplitude of a sphere or of the core-shell system, because of the high monodispersity of the samples (this is in contrast to a paper by Winnik et al. [14]).

The scattering amplitude Φ_s of N independently scattering solid spheres of the electron density ρ_s, distributed in a dispersion medium of the electron density ρ_D is given by

$$\Phi_s(\Delta\rho, R, h) = 4\pi N\Delta\rho \frac{\sin (hR) - hR \cos (hR)}{h^3} , \quad (2)$$

where R is the particle radius and $\Delta\rho = \rho_s - \rho_D$ is the contrast, respectively. The experiments were carried out at low polymer concentrations. Hence, inter-particle interferences can be neglected. Therefore, the scattering intensity I (h) can be computed from the scattering amplitude $\Phi(h)$ according to

$$I(h) = \Phi^2(h) . \quad (3)$$

This scattering intensity profile will be constant for very small-wave vectors h, as seen in Fig. 2.

The experimentally observed scattering curves exhibit the same shape and the same limiting behavior as calculations predict (Fig. 3 and 4). Differences arise from the incomplete desmearing of the experimental data, which were obtained using a Kratky camera.
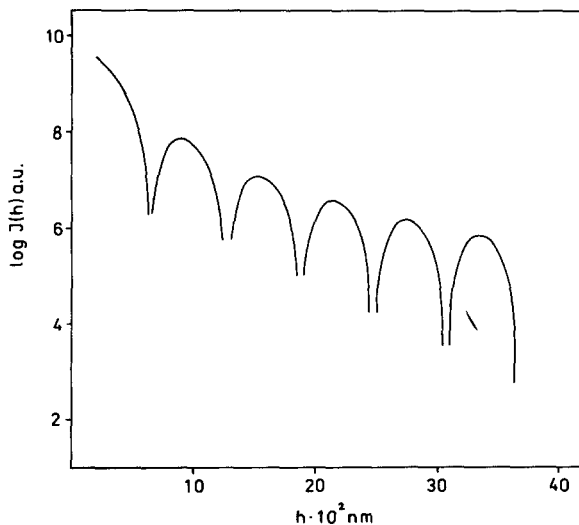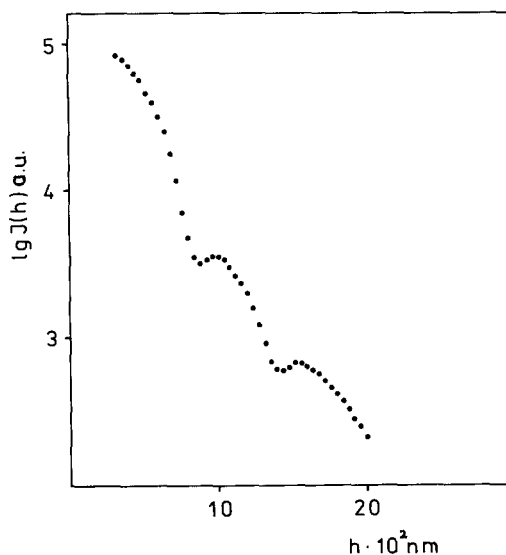

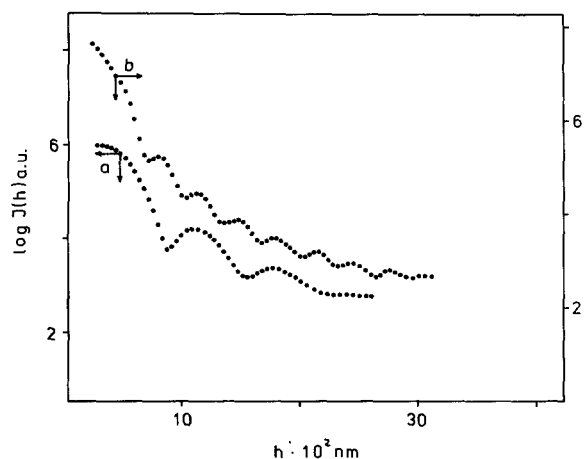Fig. 3. Experimental scattering curve for a PS latex (see Table 1)

Fig. 4. Experimental scattering curves for PMMA latexes: a) PMMA 1 b) PMMA 2 (see Table 1)

The radii of the particles recalculated from the scattering intensity profile are listed in Table 1. If one takes into consideration that the light scattering method (turbidity) has an uncertainty of about 8 %, the agreement of the radii obtained by the different methods is quite good. The x-ray scattering intensity profiles of the PMMA latexes are marked more distinctly than that of the PS latex because of the different scattering contrasts between the polymer and the surrounding water [ρ_D (water) = 333.6 electrons/nm^3; ρ_s (PS) = 340.0 electrons/nm^3; ρ_s (PMMA) = 383.3 electrons/nm^3].

Fig. 2. Scattering intensity as a function of the wave vector calculated for a system containing spheres of equal radius (R = 52.5 nm; see the PS latex)

Table 1. Particle size from light scattering and x-ray scattering

Latex	Particle diameter (nm)	
	Light scattering	SAXS
PS	101	105 +/− 1.5
PMMA 1	101	98 +/− 2.0
PMMA 2	197	188 +/− 3.0

For the general case of a core-shell system, the scattering amplitude $\Phi_{cs}(h)$ can be derived from Eq. 2 by superposition

$$\Phi_{cs}(h) = \Phi_s(\Delta\rho_2, R_2, h) - \Phi_s(\Delta\rho_2 - \Delta\rho_1, R_1, h) , \qquad (4)$$

with R_2 being the outer shell radius, R_1 the core radius, $\Delta\rho_2$ the contrast of the shell polymer with respect to the dispersion medium, and $\Delta\rho_1$ the contrast of the core polymer with respect to the dispersion medium. For $\Delta\rho_1 = 0$, one yields the known scattering amplitude for a system of hollow shell spheres [15].

The resulting profile for a system of a hollow shell with an inner radius of 52.0 nm and an outer radius of 66.0 nm (i.e., a shell thickness of 14.0 nm) is plotted in Fig. 5. The difference in the scattering profiles between spherical and hollow shell systems is obvious from the position of the minima. Scattering

curves, like that in Fig. 5, can be obtained from SANS experiments if the core scattering contribution is matched (e.g., by a mixture of H_2O and D_2O) [5, 6, 11].

In SAXS experiments, a simple matching of the core scattering contribution is impossible. The addition of a contrast enhancing agent would result in particle swelling, and the original size and structure would he changed. The use of marked monomers (e.g., with heavy metals) in the second stage would change the reaction kinetics, and then a direct comparison with real systems would be questionable. Therefore, in real core-shell systems, one has to take into account the scattering contribution of the core. In this case, the different scattering densities of the core and the shell polymer must be considered in order to calculate the intensity profile.

In the special case of PS/PMMA core-shell particles, the differences between a hollow shell scattering profile and the complete core-shell scattering profile cannot be seen by the eye in the scale of Fig. 5. Hence, the resulting scattering intensity profile according to Eq. 4 is qualitatively similar to the profile plotted in Fig. 5, because of the small scattering contribution of the core. The quantitative differences could be seen in a more extended scale.

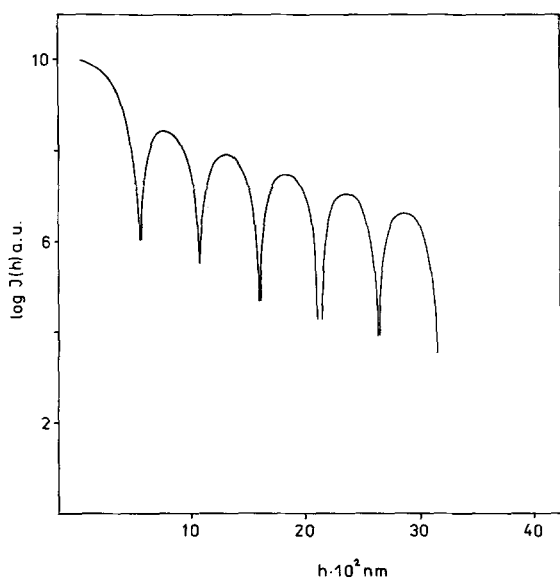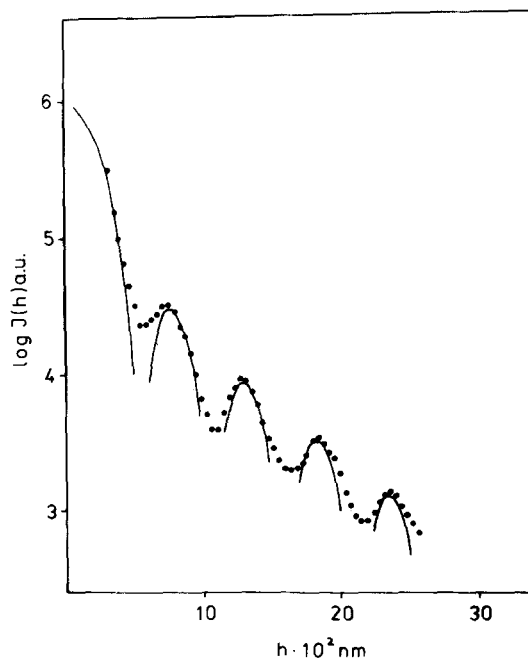The scattering intensity profile of the PS/PMMA two-stage emulsion polymers is plotted in Fig. 6. The

Fig. 5. Scattering intensity as a function of the wave vector for a system containing hollow shells of equal size according to Eq. (4), (inner radius: R_1 = 52.0 nm; outer radius: R_2 = 66.0 nm)

Fig. 6. Experimental scattering curve for a PS/PMMA core-shell latex (●) (− best fit model curve; see text)

steep increase of the curve at small-wave vectors is due to some coagulum during the second polymerization step. This coagulum influences the scattering curve in the limit $h \rightarrow 0$. The fitting of the experimental data (for larger h) with a simple sphere scattering is impossible. The best fit was made using the scattering amplitude of a complete core-shell system and inserting a core diameter of $R_1 = 52.0$ nm and a shell thickness of $(14.0 +/- 1.0)$ nm.

From the chemical composition of the latex, a shell thickness of about 16 nm can be estimated. This is in good agreement with the SAXS result. The difference may arise from the fact that, in Eq. 4, a step-wise density profile is assumed, whereas in reality the concentrations of the core and of the shell polymer should monitonically change inside an interfacial layer between both polymers. This interfacial layer is in the order of a few nm as indicated by the small difference of the shell thickness from SAXS and chemical composition, as well as by infrared spectroscopic [16] and DSC-investigations [6] of core-shell latexes. The SAXS results discussed confirm the expectation that, under the experimental conditions applied in the reaction runs, the emulsion polymerization process takes place in a small surface layer region of the polymer particles during the period of particle growth.

References

1. Keusch P, Prince J, Wiliams D J (1973) J Macromolec Sci - Chem A7:623
2. Kamei S, Okubo M, Matsumoto T (1980) J Polym Sci, A, Polym Chem Ed 16:3109
3. Okubo M, Yamada A, Matsumoto T (1980) J Polym Sci, Polym Chem Ed 16:3219
4. Ford JR, Rowell RL, Bassett D R (1981) In: Bassett DR, Hamielec AE (eds) Emulsion Polymers and Emulsion Polymerization, ACS, Washington, p. 279
5. Wai MP, Gelman RA, Fatica MG, Hoerl RH, Wignall GD (1987) Polymer 28:918
6. Tanneberger H, Bittrich H-J, Steinau U-J, Hergeth W-D (1987) Wiss Z TH Leuna-Merseburg 29:721
7. Zecha H, private communication
8. Guinier A, Fournet G (1955) Small-Angle Scattering of X-Rays, John Wiley, New York and Chapman & Hall, London, pp. 111
9. Schmutzler K (1982) Acta Polymerica 33:455
10. Hergeth W-D, Schmutzler K (1985) Acta Polymerica 36:472
11. Hergeth W-D, Eichhorn F, Bittrich H-J, Schlenker S, Steinau U-J, Schmutzler K (1989) Polymer 30:1913
12. Hergeth W-D, Starre P, Schmutzler K, Wartewig S (1988) Polymer 29:1323
13. Hergeth W-D, Bittrich H-J, Steinau U-J, Schmutzler K (1987) Lecture, 31st IUPAC Macromolecular Symposium, Merseburg, 1987, Microsymposium VI, p. 34
14. Winnik MA, Williamson B, Russell TP (1987) Macromolecules 20:899
15. Pecora R, Aragon SR (1974) Chem Phys Lipids 13:1
16. Lange J, Hergeth W-D, Wartewig S (1988) Acta Polymerica 39:479

Authors' address:

Dr. W.-D. Hergeth
Technical University Merseburg
Otto-Nuschke-Straße
4200 Merseburg, GDR